Electronic Supplementary Material (ESI) for Chemical Communications.

A novel NiVP/Pi based flexible sensor for direct electrochemical ultrasensitive detection of cholesterol

Experimental section

Materials and reagents

All chemicals and reagents were of analytical grade and used as received without further purification. Potassium dihydrogen phosphate (KH_2PO_4), dipotassium hydrogen phosphate (K_2HPO_4), urea (CH_4N_2O) and isopropanol (C_3H_8O) were procured from Merck. 0.1 M PBS was prepared from the stock solutions of 0.1 M KH_2PO_4 and 0.1 M K_2HPO_4. Nickel chloride hexahydrate ($NiCl_2.6H_2O$, 97%), ammonium metavanadate (NH_4VO_3, 99%), red phosphorus (98%), ammonium fluoride (NH_4F, 98%, crystalline), potassium hydroxide pellets (KOH) and sodium chloride (NaCl) were purchased from Loba Chemie. Sodium hydroxide (NaOH) was obtained from Alfa Aesar. Glucose ($C_6H_{12}O_6$, >99%), dopamine hydrochloride ($C_8H_{11}NO_2.HCl$, >99%), ascorbic acid ($C_6H_8O_6$, 99%) and uric acid ($C_5H_4N_4O_3$, >99%) were from Sigma-Aldrich. Deionized water obtained from a Millipore system has been used throughout the experiments. (>12 MΩ cm^{-1}).

Synthesis of NiVP/Pi

NiVP/Pi catalyst material was synthesized using previously reported literature.[1] Briefly, the synthesis process of NiVP/Pi material involves two-step, wherein the first step involves the formation of nickel vanadium layer double hydroxides through hydrothermal reaction. Initially, 35 mL aqueous mixture of $NiCl_2.6H_2O$ and NH_4VO_3 (2:1 molar ratio) were kept under stirring for 10 min. Later, 18 mmol of urea and ammonium fluoride was added to the reaction mixture, stirred for 30 minutes for homogeneity and solution

was heated hydrothermally at 120 °C for 6 h in Teflon-lined autoclave. After cooling, the precipitate of nickel vanadium layer double hydroxides ($NiV(OH)_2$) was washed with (1:1) water and ethanol mixture (3×10 mL) and dried overnight at 60 °C. The second step involves the phosphorization reaction, in which as obtained brown $NiV(OH)_2$ (0.300 g) was mixed with 0.100 g of red phosphorous in 10 mL water and transferred to a microwave vial. Before irradiation, the solution mixture was purged with N_2 gas for 10 minutes and it was irradiated in a Multiwave Pro instrument (Anton Paar) at 100 °C with a 15 min ramp and held for 30 min at 100 °C, under a limiting pressure of 18 bar at 600 watt by controlled temperature programming. The obtained precipitate of NiVP/Pi was filtered and washed (3×30 mL) with deionized water and dried at 60 ˚C in an oven. Likewise, NiP/Pi and VP/Pi was synthesized under similar reaction conditions using only $NiCl_2.6H_2O$ and NH_4VO_3, respectively.

Physical characterization

The X-ray powder diffraction (XRD) patterns of NiVP/Pi were collected using PANalytical X'PERT pro diffractometer using Cu K-α radiation (λ=0.1542 nm, 40 KV, 40 mA) in the range of 10-80° at a scan speed of 2° per minute. The morphology and elemental distribution of the catalyst was recorded using field scanning microscopy (FESEM; SUPRA 55 VP- 4132 CARL ZEISS). Further, high resolution transmission electron microscopy (HR-TEM) was employed to characterize in depth morphology using FEI Tecnai (G2 F20), Netherlands operating at 200 keV. X-ray photoelectron spectroscopy (XPS) measurements were obtained using Thermo scientific NEXSA surface analysis (working at 72 W, 12000 V), Al Kα radiation (1486.6 eV) under ultrahigh vacuum (UHV 8-10 mbar). The spectra were calibrated with respect to C (1s) peak at 284.5 eV with a precision of ±0.2 eV.

Electrochemical measurements

All the electrochemical experiments were performed using three-electrode system assembled in a single compartment. Cyclic voltammetry (CV), chronoamperometric and electrochemical impedance

measurements (EIS) experiments were conducted on a Bio-Logic (VSP 300 electrochemical workstation at room temperature. 0.1 M NaOH was used as the electrolyte and catalyst modified Ni foam ((thickness: 1.6 mm, 0.12 cm^2) used as working electrode (WE), Ag/AgCl/3 M KCl double junction as a reference electrode (RE) and Pt wire as a counter electrode (CE).

For slurry preparation, 1.25 mg of the catalyst sample was dispersed in 500 μL of solution containing isopropyl alcohol (IPA, 100 μL) and Millipore water (400 μL, 12 MΩ), and sonicated for about 30 min. Once a homogeneous slurry was attained, the working electrode was prepared by drop-casting 20 μL (50 μg) of obtained sample slurry on the Ni foam for performing the electrochemical measurements. Prior to use, Ni foam was pretreated with 1 M HCl solution and washed with ethanol and distilled water, respectively. Electrochemical impedance measurements (EIS) were conducted at a DC voltage of 0.54 V over a frequency range between 10 mHz to 3 MHz. Each experiment has been repeated at least 4-5 times to ensure reproducibility.

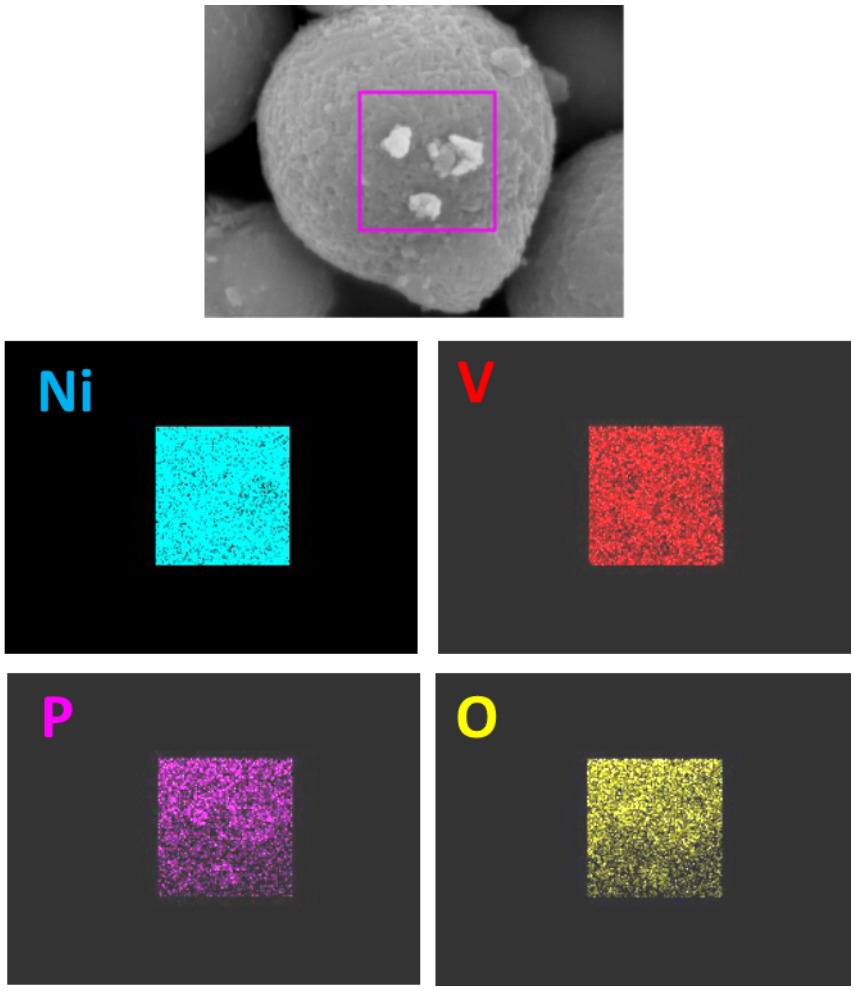

Figure S1. EDS dot mapping of Ni, V, P and O elements in NiVP/Pi catalyst.

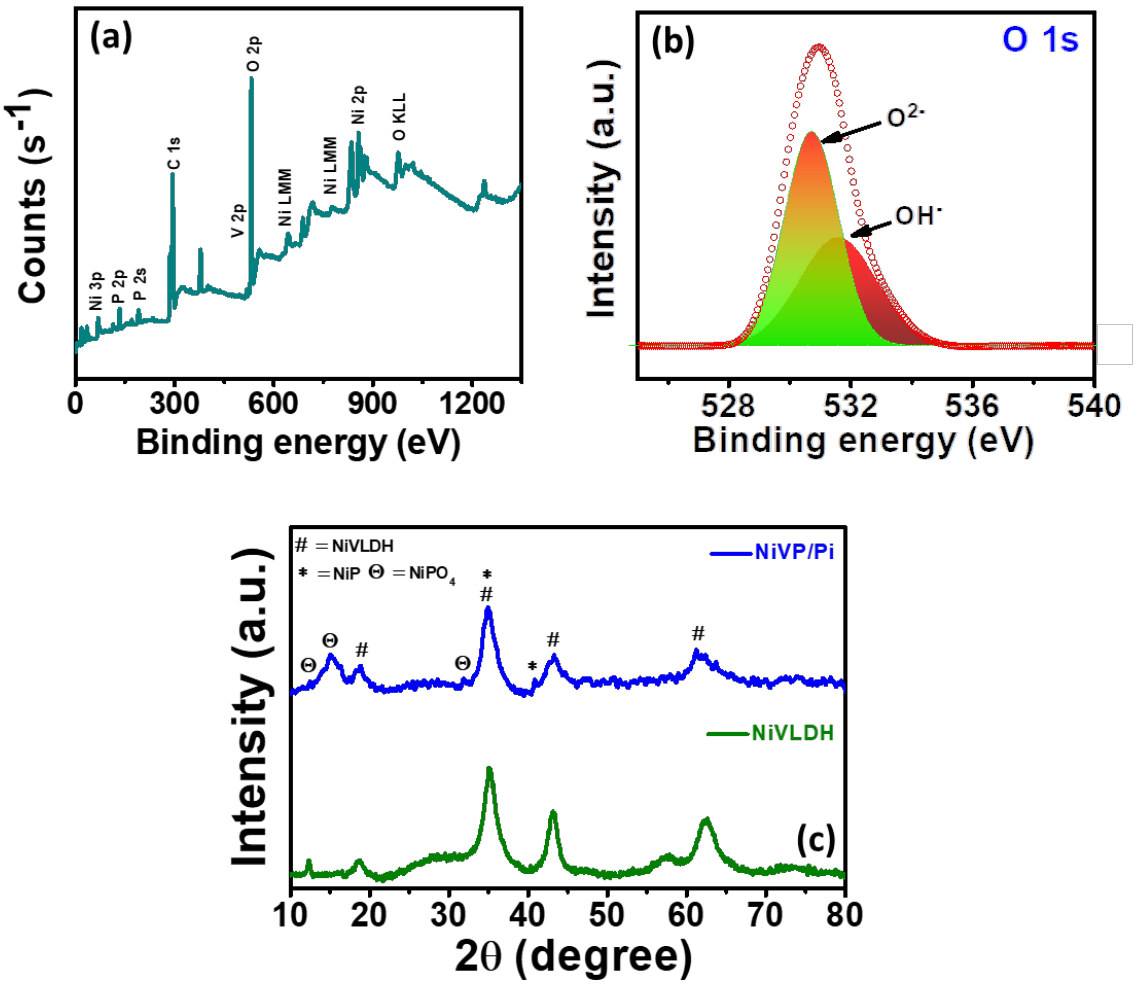

Figure S2. (a) XP survey spectra of NiVP/Pi catalyst, (b) O 1s XP spectra of NiVP/Pi catalyst and (c) XRD patterns of NiVP/Pi and NiVLDH catalyst.

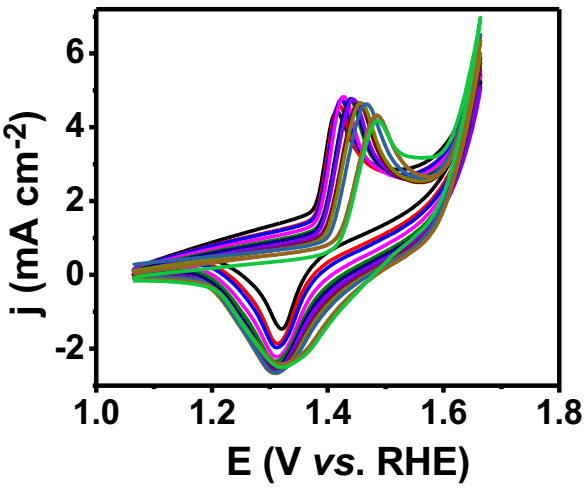

Figure S3. CV response of bare Ni foam in 0.1 M NaOH electrolyte containing various conc. of cholesterol at a scan rate of 5 mV s^{-1}, CE: Pt wire, RE: double junction Ag/AgCl/3 M KCl.

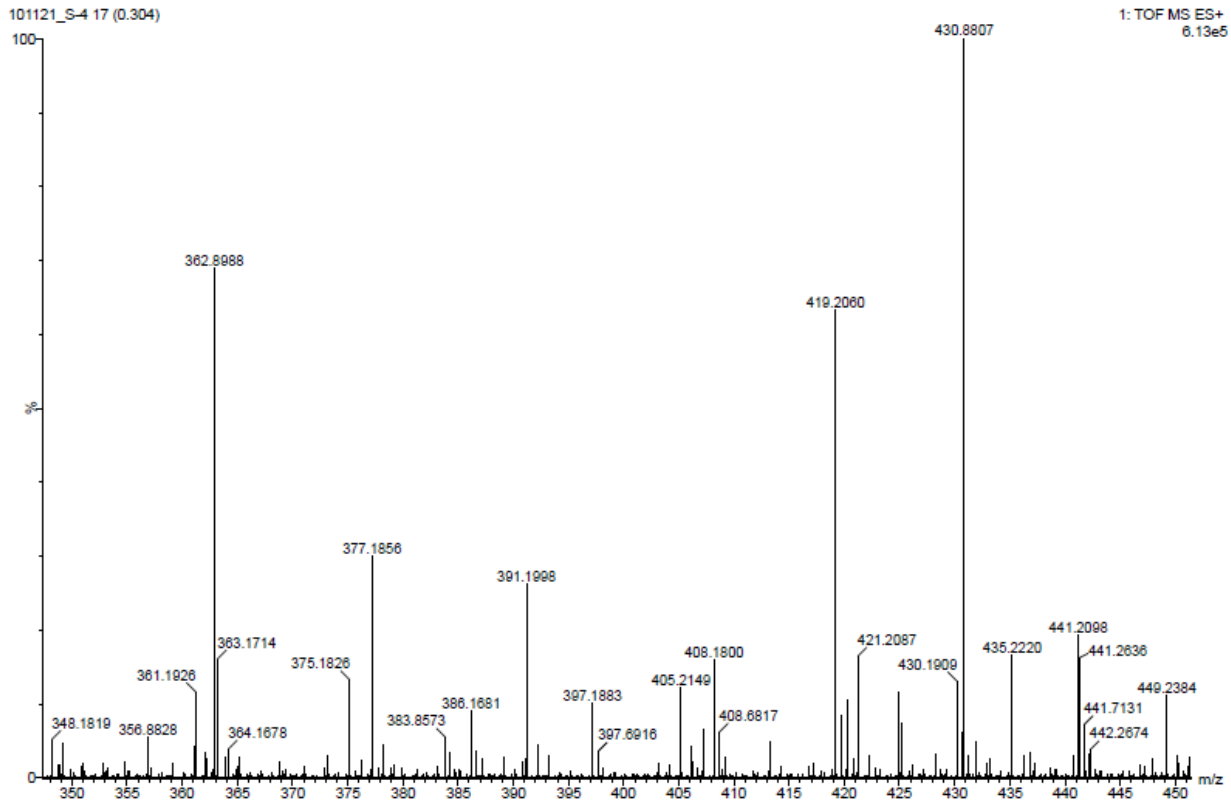

Figure S4. HRMS data collected after electrochemical oxidation of cholesterol over NiVP/Pi catalyst in 0.1 M NaOH electrolyte.

	Cholesterol	**Cholest-4-en-3-one**	**7-ketocholesterol**	**Cholestane-3-β-5-α-6-β-triol**
Parent peak	386.1	383.8	--	419.2
Adduct with Na^+	408.81	--	--	442.2
Adduct with Na^+ - 2H	--	405.2	421.2	441.2

HR-MS analysis: To understand the product of the electrooxidation of cholesterol, the LC-MS measurement was accomplished using the electrolyte. CV measurement was performed with NiVP/Pi catalyst in 0.1 M NaOH electrolyte containing 500 µM of cholesterol. Fig. S4 clearly demonstrates the formation of oxidized products, describing the electro-oxidation of cholesterol.

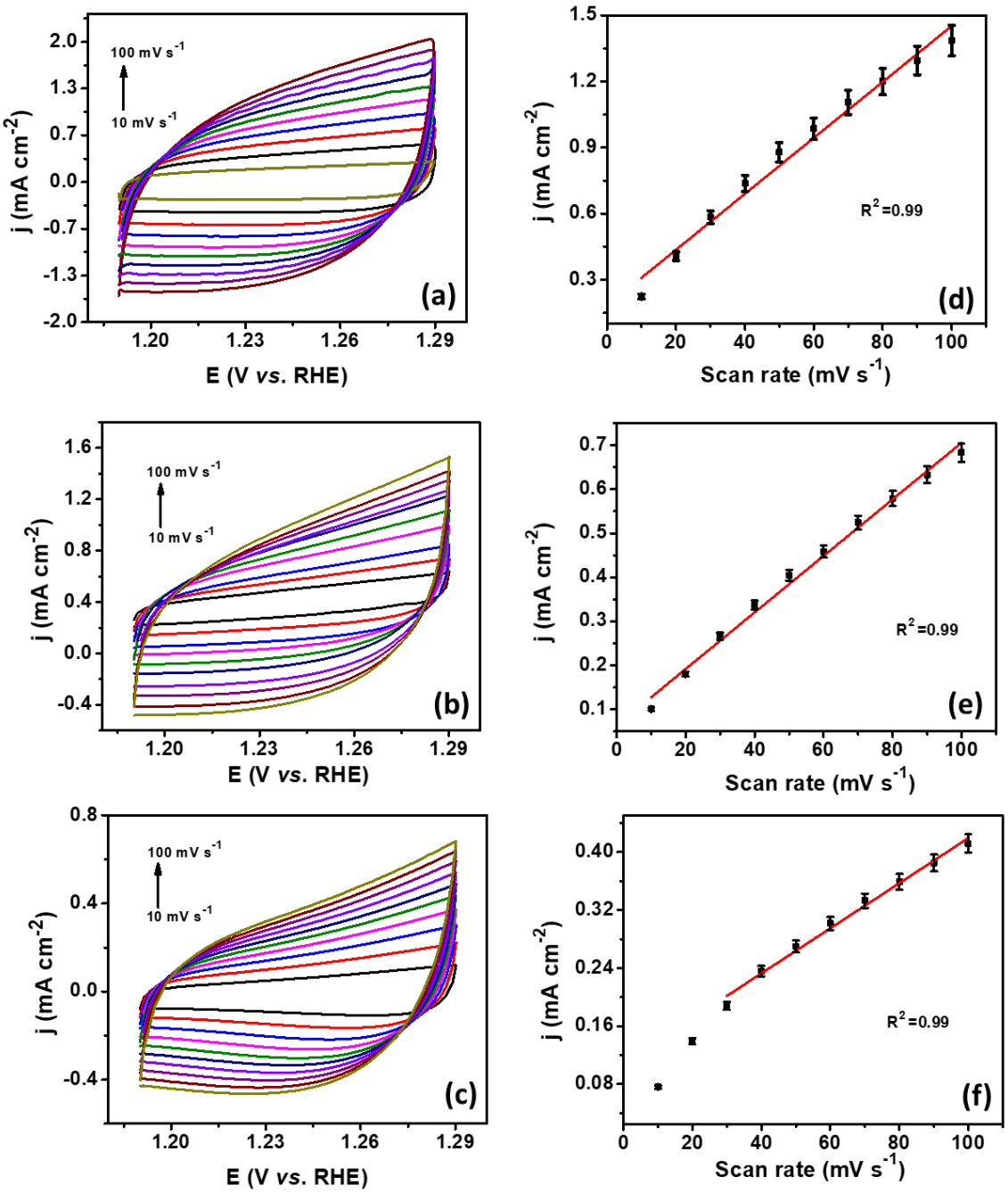

Figure S5. Cyclic voltammograms for (a) NiVP/Pi, (b) NiP/Pi and (c) VP/Pi catalyst at varying scan rates in the non-faradic potential region and inset; corresponding average current density versus scan rate in the presence of 5 mM cholesterol CE: Pt wire, RE: double junction Ag/AgCl/3 M KCl.

Electrochemical surface area (ECSA)

The electrochemical surface area of the catalyst was determined by computing the double-layer pseudo-capacitance (*Cdl)* in the non-faradaic region in 0.1 M NaOH with an analyte solution. Cyclic voltammetry was performed in non-faradic region in potential range from 0.32 V to 0.42 V *vs.* Ag/AgCl/3 M KCl double junction at various scan rates (10 to 100 mV s^{-1}). Thereafter, slope of the plot between averaged current density of anodic and cathodic current (Ia+Ic)/2 (where, 'a' denotes anodic current and 'c' is for cathodic current) *vs*. the scan rate at 0.37 V (*vs.* Ag/AgCl/3 M KCl) was calculated, which gives pseudo-capacitance. C_{dl} on dividing with the specific capacitance (C_s) of the flat standard surface (20-60 μF cm^{-2}), which is considered to be 40 μF cm^{-2}, gives electrochemical surface area (ECSA).[1]

ECSA calculation:

ECSA = ***Cdl*** / ***Cs***

Table S1: Electrochemical surface area (ECSA) analysis.

S.No.	Catalyst	C_{dl} (μF) at 0.37 V (*vs.* Ag/AgCl/3 M KCl)	ECSA (cm^2)
1.	NiVP/Pi	1906.5	47.5
3.	NiP/Pi	963	24
4.	VP/Pi	466.5	11.6

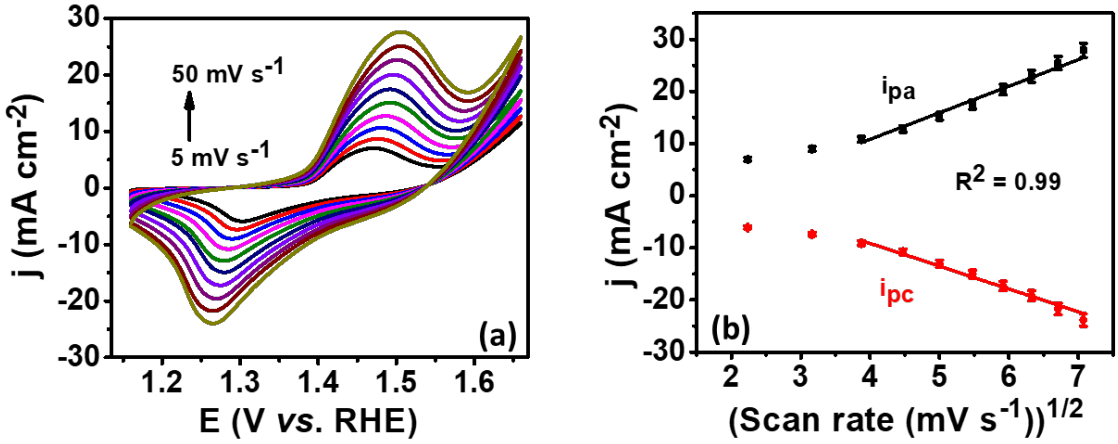

Figure S6. (a) Cyclic voltammograms of NiVP/Pi catalyst at various scan rates, and (b) corresponding average current density *vs.* scan rate in 0.1 M NaOH electrolyte containing 10 µM cholesterol CE: Pt wire, RE: double junction Ag/AgCl/3 M KCl.

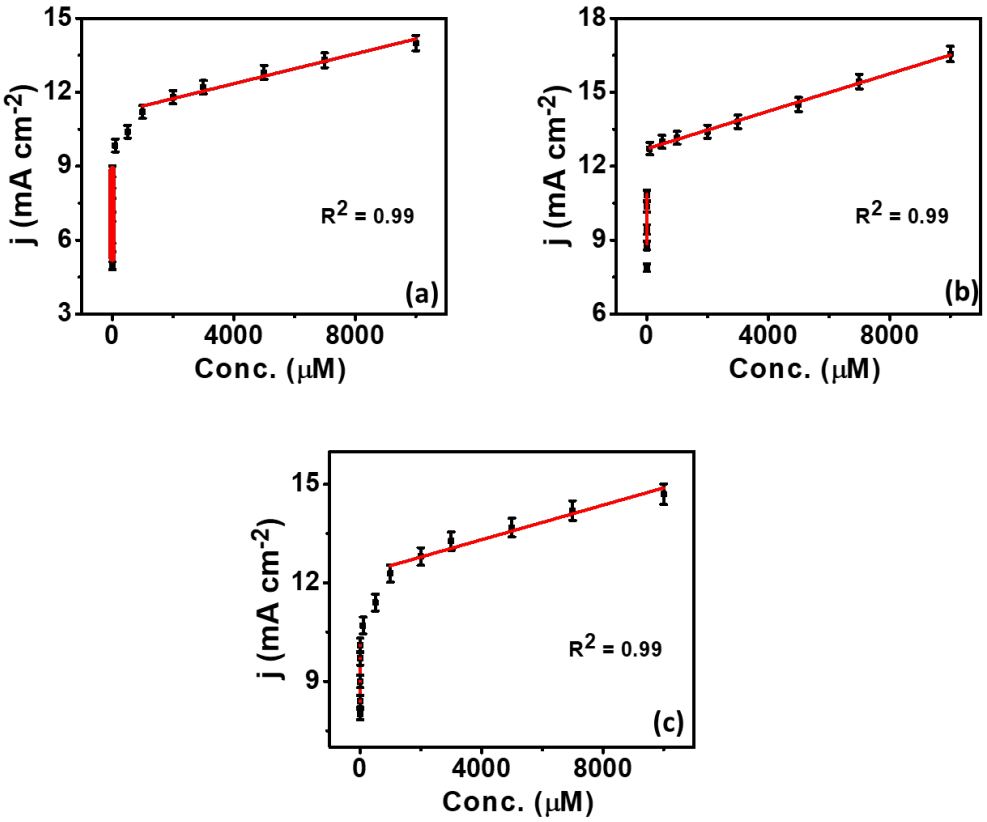

Figure S7. Plot of current density *vs*. concentration of cholesterol for NiVP/Pi over paper electrode in (a) 0.1 M NaOH electrolyte, (b) 0.1 M PBS electrolyte (pH =7.4)) at various conc. of cholesterol, (c) at various conc. of blood serum sample, extracted from Fig. 2.

Furthermore, in order to authenticate the pertinency of the proposed sensor in practical applications for the detection of cholesterol, NiVP/Pi catalyst was analyzed in real sample using human blood serum via standard addition method. Blood serum sample was injected in 0.1 M NaOH electrolyte and known amounts of cholesterol in the test solution was added. The obtained results are tabulated in Table S2 (SI). The recovery of the spiked sample was found from 97 to 106, which governs the applicability of the proposed sensor for real time analysis as well.

Table S2. Human serum sample analysis with NiVP/Pi modified electrode.

Sample	**Actual Conc.**	**Conc. (Added)**	**Conc. (found)**	**Recovery (%)**
1.	5 μM	100 μM	102 μM	97
2.	5 μM	200 μM	202 μM	98.5
3.	5 μM	300 μM	325 μM	106
4.	5 μM	500 μM	516 μM	102

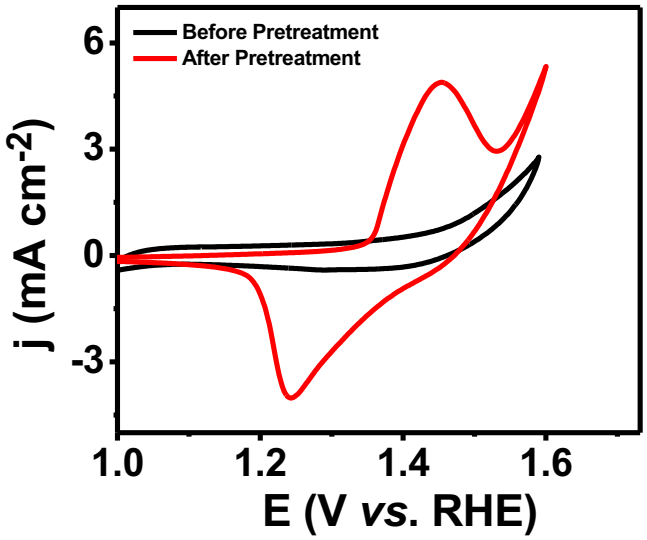

Figure S8. Cyclic voltammograms of pretreated NiVP/Pi over paper electrode in 0.1 M PBS electrolyte (pH =7.4)); CE: Pt wire, RE: double junction Ag/AgCl/3 M KCl.

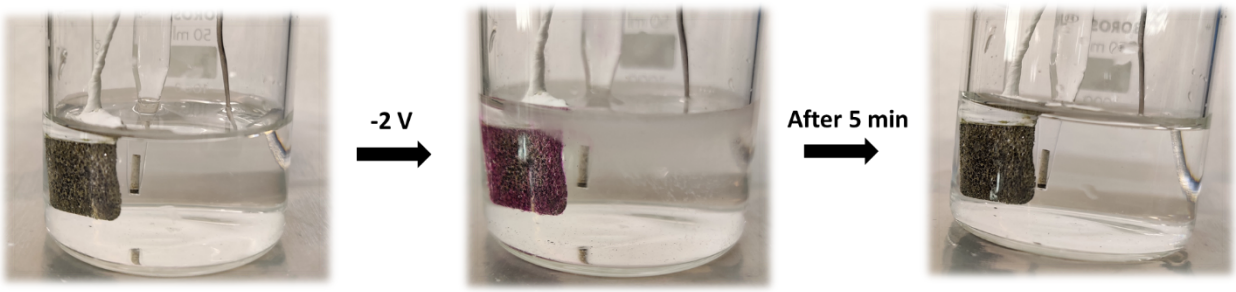

Figure S9. Photographs displaying pH change after applying -2 V in 0.1 M PBS (pH 7.4) solution containing 5 µL of 5% phenolphthalein (in ethanol) in the electrochemical cell; CE: Pt wire, RE: double junction Ag/AgCl/3 M KCl.

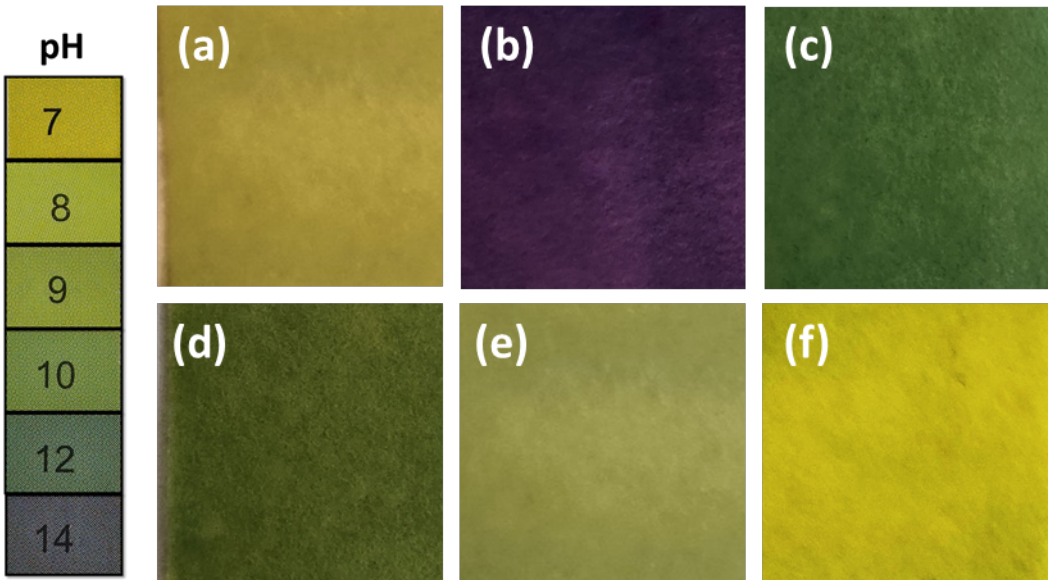

Figure S10. The color change on pH test strips of solution samples under steady conditions at different time, (a) before pretreated, (b-f) after pretreated for 0.5 min, 1 min, 2 min, 5 min, 7 min.

The local pH at the electrode/electrolyte interface was adjusted by applying a preconditioning potential (-2 V) on the NiVP/Pi electrode (Fig. S8A, ESI†) and the pH change at the electrode-electrolyte interface was demonstrated by the appearance of pink color from colorless due to phenolphthalein addition during the pretreatment process, suggesting the pH change from neutral to alkaline (Fig. S8B, ESI†). Interestingly, after pretreatment, the pH near the working electrode gradually decreased and it was shown by the color change from pink back to colorless because of diffusion of ions leading to neutralization with phosphate buffer. It was well supported by pH strip studies showing change of pH from 7.4 to about 13 at different time intervals using a glass capillary near working electrode (Fig. S8C, ESI†). Furthermore, 30 seconds was chosen as appropriate time period for the change of pH to ≈14, as investigated by pH meter studies, which led to alkaline environment for nonenzymatic detection of cholesterol.

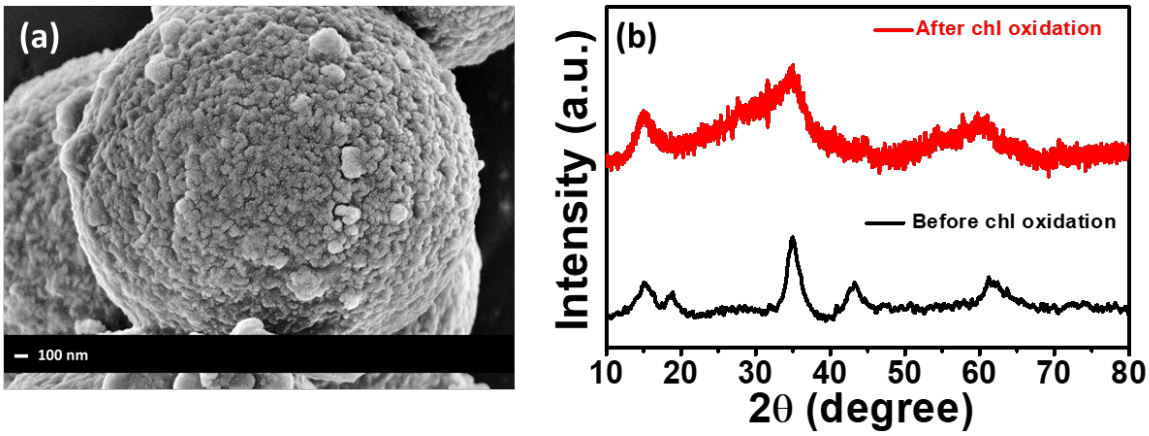

Figure S11. (a) SEM images and (b) XRD pattern of NiVP/Pi catalyst after electrochemical cholesterol oxidation.

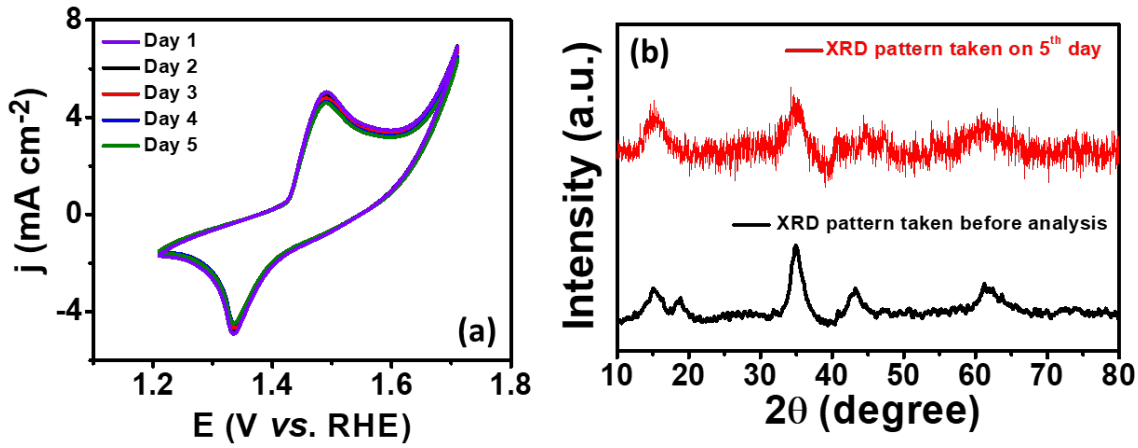

Figure S12. (a) Cyclic voltammograms of NiVP/Pi catalyst coated over paper electrode at 5 mM of cholesterol in 0.1 M PBS electrolyte (pH =7.4)); CE: Pt wire, RE: double junction Ag/AgCl/3 M KCl and (b) XRD patterns of NiVP/Pi catalyst before and after 5 days of analysis of electrochemical cholesterol oxidation.

Table S3. Comparison of analytical performance of cholesterol sensor with various modified electrodes reported previously.

Catalyst	Concentra-tion range	Limit of detection	Sensitivity	Selectivity	Stability	Real sample analysis	Ref.
Cu_2S NRS/CRIE	0.01 – 0.68 mM	0.1 µM	62.5 µA mM^{-1}	No interference	92% retention after 30 days	_	2
Au NPs/rGO-PAMAM-Fc	0.0004 – 15.36 mM	0.01 µM	_	No interference	80% retention on 12^{th} repeated measurement	Human blood serum	3
Chox/MoS_2-AuNPs/GCE	0.5 – 48 µM	0.26 ± 0.015 µM	4460 µA mM^{-1} cm^{-2}	Little interference	Upto 14 days	Raw egg yolk and pork sample	4
Cu_2O-TiO_2	24.4 – 622 µM	0.05 µM	6034.04 µA mM^{-1} cm^{-2}	Negligible interference	84% after 10 CV cycles	Human blood serum	5
α-Fe_2O_3	0.1-8.0 mM	0.018 mM	78.56 µA mM^{-1} cm^{-2}	Negligible interference	97% retention after 2 weeks	Human blood serum	6
CuO-NPs	1 µM to 15 µM	0.43 µM	1098.37 µA mM^{-1} cm^{-2}	Negligible interference		Human blood serum	7
ZnO nanoparticle	0.001 – 0.5 µM		23.7 µA mM^{-1} cm^{-2}				8
NiO/CVD-grown graphene	2 – 40 µM	0.13 µM	40.6 mA μM^{-1} cm^{-2}	Negligible interference	2 days	Milk sample	9
micro-needle patch and nanoporous platinum (NPt) sensing electrodes	-	-	305 nA mM^{-1} cm^{-2}	-	-	-	10
MIP-AuNPs-PDA-DGr/GCE	10^{-18} - 10^{-13} M	3.3×10^{-19} M	–	_	97.4% retention after 40 days	Human blood serum	11
PANInf-GMF	1.93 to 464.04 mg dl^{-1}	1.93 mg dl^{-1}	0.101 µA mg^{-1} dl cm^{-2}	No interference	up to 12 weeks	-	12
α-Fe_2O_3	0.1-8.0 mM	0.018 mM	78.56 µA mM^{-1} cm^{-2}	Negligible interference	97% retention after 2 weeks	Human blood serum	6

ZnO@ZnS	0.4 – 3.0 mM	0.02 mM	52.67 mA M^{-1} cm^{-2}	< 5% interference	5% after 30 days	–	13
Au-/nPts	-	0.015 mM	226.2 µA mM^{-1} cm^{-2}	No interference	_	_	14
Ru-Pi-PPy/CFP	0.16 - 20 nM	0.54×10^{-10} M	19988 µA μM^{-1} cm^{-2}	3% interference	30 days	Human blood serum	15
Cu-Ni bimetal-dispersed carbon nanofiber/polymer nanocomposite (BMCP)-based electrode	0.04 - 600 mg dL^{-1}	0.002 mg dL^{-1}	226.30 µA mM^{-1} cm^{-2}	Small interference by AA	8 months	Human blood serum	16
CoMnHCF	50 - 150 µM	30 µM	385 mA M^{-1} cm^{-2}	Negligible interference	_	_	17
	150 -1000 µM		80 mA M^{-1} cm^{-2}				
GO&CHER&CHOD/Au NPs/SPE	0.01 - 5000 µgmL^{-1}	0.001 µgm L^{-1}	0.084 µA cm^2 µgmL^{-1}	Little interference	86.58% retention after 15 days	_	18
MB/BCD/Fe_3O_4/SPCE	0 - 150 µM	2.88 µM	0.015 µA μM^{-1}	Negligible interference	_	Milk sample	19
Grp/β-CD/Methylene Blue	0.01 - 0.10 mM	–	0.01 µA μM^{-1}	Negligible interference	100 CV cycles	_	20
ChEt−ChOx/n-$NiFe_2O_4$−CH/ITO	5 - 400 mg dL^{-1}	24.46 mg dL^{-1} cm^{-2}	1.73 µA (mg dL^{-1} cm^{-2})$^{-1}$	Insignificant interference	78% retention after 90 days	Human blood serum	21
Pt-NCs	2 - 486 µM	2 µM	132 µA mM^{-1} cm^{-2}	Suppressed interference at 0.3 V	79% retention after 3 weeks	Human blood serum	22
NRs-NiO	1.5 - 10.3 mM	_	0.12 mA mM^{-1} cm^{-2}	Negligible interference by UA	95% retention after 3 weeks	_	23
β-CD@N-GQD	0.5 - 100 µM	80 nM	–	Limited interference	87% retention after 28 days	Serum sample	24
GC/Chi-$Ni(OH)_2$/Chox/NF	0.45 - 10 mM	49 µM	–	–	3 months	–	25
PANI/MWCNTs/Starch	0.032 - 5 mM	0.01 mM	800 µA mM^{-1} cm^{-2}	Higher selectivity than AA	More than 3 years	Cow milk	26
AuNPs–MWNTs/GCE	10^{-13} - 10^{-9} M	3.3 10^{-14} M	–	Low interference	91.68% retention after one month	_	27

PEDOT/TA composite	3 µM - 1 mM	0.95 µM	–	Nearly selective	87% retention after one month	Egg yolk sample	28
Au/CdS QDs/TNTs	0.024 - 1.2 mM	~0.012 µM	10,790 µA mM^{-1} cm^{-2}	Negligible interference	92.7% retention after 4 weeks	Human blood serum	29
Au NPs	5–5000 µg/mL	3.0 µg/mL		Negligible interference	25% loss after 10 measurements		30
Oxidized Zn–In nanostructure	0.5 mM – 09 mM		81 µA mM^{-1} cm^{-2}				31
PVIM–Co_5POM/MNC	1 fM - 200 nM; 0.5 µM - 5 mM	1 fM	210 µA μM^{-1} cm^{-2} 64 µA μM^{-1} cm^{-2}	Small interference in presence of AA	100 consecutive CV cycles	Human blood serum	32
NiVP/Pi	**1 nM - 10 µM;** **100 µM - 10 mM**	**1 aM**	**5510.18 µA μM^{-1} cm^{-2}** **36.8 µA μM^{-1} cm^{-2}**	**Negligible interference**	**100 consecutive CV cycles**	**Human blood serum**	**This Work**

Reference:

1. N. Thakur, D. Mandal and T. C. Nagaiah, *J. Mater. Chem. B*, 2021, **9**, 8399-8405.
2. R. Ji, L. Wang, G. Wang and X. Zhang, *Electrochim. Acta*, 2014, **130**, 239-244.
3. J. Zhu, Z. Ye, X. Fan, H. Wang, Z. Wang and B. Chen, *Int. J. Nanomedicine*, 2019, **14**, 835.
4. X. Lin, Y. Ni and S. Kokot, *Sens. Actuators B Chem.*, 2016, **233**, 100-106.
5. N. Khaliq, M. A. Rasheed, G. Cha, M. Khan, S. Karim, P. Schmuki and G. Ali, *Sens. Actuators B Chem.*, 2020, **302**, 127200.
6. A. Umar, R. Ahmad, S. W. Hwang, S. H. Kim, A. Al-Hajry and Y. B. Hahn, *Electrochim. Acta*, 2014, **135**, 396-403.
7. Q. Wu, L. He, Z. W. Jiang, Y. Li, Z. M. Cao, C. Z. Huang and Y. F. Li, *Biosens. Bioelectron.*, 2019, **145**, 111704.
8. A. Umar, M. Rahman, M. Vaseem and Y.-B. Hahn, *Electrochem. Commun.*, 2009, **11**, 118-121.
9. A. Rengaraj, Y. Haldorai, C. H. Kwak, S. Ahn, K.-J. Jeon, S. H. Park, Y.-K. Han and Y. S. Huh, *J. Mater. Chem. B*, 2015, **3**, 6301-6309.
10. H. Yoon, S. Lee, J. Park, S.-J. Paik and M. G. Allen, SENSORS, 2014 IEEE, 2014.
11. H. Yang, L. Li, Y. Ding, D. Ye, Y. Wang, S. Cui and L. Liao, *Biosens. Bioelectron.*, 2017, **92**, 748-754.
12. G. Lakshmi, A. Sharma, P. R. Solanki and D. Avasthi, *Nanotechnology*, 2016, **27**, 345101.

13. A. K. Giri, C. Charan, A. Saha, V. K. Shahi and A. B. Panda, *J. Mater. Chem. A*, 2014, **2**, 16997-17004.
14. Y.-J. Lee and J.-Y. Park, *Biosens. Bioelectron.*, 2010, **26**, 1353-1358.
15. K. Akshaya, A. Varghese, M. Nidhin and L. George, *J. Electrochem. Soc.*, 2019, **166**, B1016.
16. P. K. Bairagi and N. Verma, *J. Electroanal. Chem.*, 2018, **814**, 134-143.
17. M. Antuch, Y. Matos-Peralta, D. Llanes, F. Echevarría, J. Rodríguez-Hernández, M. H. Marin, A. M. Díaz-García and L. Reguera, *ChemElectroChem*, 2019, **6**, 1567-1573.
18. Y. Huang, J. Tan, L. Cui, Z. Zhou, S. Zhou, Z. Zhang, R. Zheng, Y. Xue, M. Zhang and S. Li, *Biosens. Bioelectron.*, 2018, **102**, 560-567.
19. S. J. Willyam, E. Saepudin and T. A. Ivandini, *Anal. Methods*, 2020, **12**, 3454-3461.
20. N. Agnihotri, A. D. Chowdhury and A. De, *Biosens. Bioelectron.*, 2015, **63**, 212-217.
21. J. Singh, A. Roychoudhury, M. Srivastava, V. Chaudhary, R. Prasanna, D. W. Lee, S. H. Lee and B. Malhotra, *J. Phys. Chem. C*, 2013, **117**, 8491-8502.
22. K. S. Eom, Y. J. Lee, H. W. Seo, J. Y. Kang, J. S. Shim and S. H. Lee, *Analyst*, 2020, **145**, 908-916.
23. M. A. Ali, P. R. Solanki, M. K. Patel, H. Dhayani, V. V. Agrawal, R. John and B. D. Malhotra, *Nanoscale*, 2013, **5**, 2883-2891.
24. A. B. Ganganboina and R.-a. Doong, *Microchim. Acta*, 2018, **185**, 526.
25. K. Selvarani and S. Berchmans, *J. Electrochem. Soc.*, 2017, **164**, H561.
26. V. Gautam, K. P. Singh and V. L. Yadav, *Anal. Bioanal. Chem.*, 2018, **410**, 2173-2181.
27. J. Ji, Z. Zhou, X. Zhao, J. Sun and X. Sun, *Biosens. Bioelectron.*, 2015, **66**, 590-595.
28. P. Thivya, R. Ramya and J. Wilson, *Microchem. J.*, 2020, **157**, 105037.
29. N. Khaliq, M. A. Rasheed, M. Khan, M. Maqbool, M. Ahmad, S. Karim, A. Nisar, P. Schmuki, S. O. Cho and G. Ali, *ACS Appl. Mater. Interfaces*, 2021, **13**, 3653-3668.
30. Y. Huang, L. Cui, Y. Xue, S. Zhang, N. Zhu, J. Liang and G. Li, *Mater. Sci. Eng. C*, 2017, **77**, 1-8.
31. S. Khan, M. A. Rasheed, A. Shah, A. Mahmood, A. Waheed, S. Karim, M. Khan and G. Ali, *Mater. Sci. Semicond. Process.*, 2021, **135**, 106101.
32. N. Thakur, M. Kumar, S. Das Adhikary, D. Mandal and T. C. Nagaiah, *Chem. Commun.*, 2019, **55**, 5021-5024.